

0017-9310(95)00064-X

The influence of surface mass flux on vortex instability of a horizontal mixed convection flow in a saturated porous medium

JIN-YUH JANG and KUN-NUN LIE

Department of Mechanical Engineering, National Cheng-Kung University Tainan, Taiwan 70101,
Republic of China

and

JING-LIN CHEN

Power Research Institute, Taiwan Power Company, Taipei, Taiwan 10325, Republic of China

(Received 30 August 1994)

Abstract—A numerical analysis is made to analyse the effect of uniform blowing or suction on the vortex mode of instability of a horizontal mixed convection boundary layer flow with a uniform free stream velocity in a saturated porous medium. The governing equations for the base flow are solved by using a suitable variable transformation and employing an implicit finite-difference Keller Box method. The stability analysis is based on the linear stability theory and the resulting eigenvalue problem is solved by the local similarity method. The results indicate that, for blowing, the Nusselt numbers are lower than those for an impermeable surface and the flow is more susceptible to the vortex instability, while the opposite trend is true for suction.

1. INTRODUCTION

The problems of vortex mode of instability in natural or mixed convection flow over a heated plate in a saturated porous medium have received considerable attention in past decades. This is primarily due to a large number of technical applications, such as fluid flow in a geothermal reservoir, separation processes in chemical industries, storage of radioactive nuclear waste materials, transpiration cooling, transport processes in aquifers, etc.

Hsu *et al.* [1] and Hsu and Cheng [2] analysed the vortex mode of instability for natural convection boundary layer flow adjacent to an impermeable surface, horizontal and inclined, in porous media. Jang and Chang [3] re-examined the same problem for an inclined plate, where both the streamwise and normal components of the buoyancy force are retained in the momentum equations. Jang and Chang [4] studied the vortex instability of horizontal natural convection in porous media resulting from combined heat and mass buoyancy effects. The effects of density extremum on the vortex instability of an inclined buoyant layer in porous media saturated with cold water were examined by Jang and Chang [5, 6]. The non-Darcian effects on the vortex instability of a horizontal natural convection flow in a high-porosity medium were investigated by Chang and Jang [7, 8].

For mixed convection boundary layer flow adjacent

to an impermeable surface, Hsu and Cheng [9] analysed the vortex instability for horizontal flow in a porous medium. Hsu and Cheng [10] applied a linear stability analysis to determine the condition of onset of vortex instability for flow over an inclined surface. Jang and Lie [11] provided new vortex instability results for small angles of inclination from the horizontal ($\phi \leq 25^\circ$) and more accurate results than reported in a previous study [10] for larger angles of inclination ($\phi > 25^\circ$). Recently, the boundary and inertia effects on vortex instability of a horizontal mixed convection flow have been examined by Lie and Jang [12].

All of the works mentioned above are conducted for flows over an impermeable surface. The free convections with blowing or suction over a vertical and a horizontal plate in a porous medium were studied by Cheng [13] and Minkowycz *et al.* [14], respectively. Lai and Kulacki [15, 16] investigated the effects of blowing or suction on mixed convection over horizontal and inclined surfaces in saturated porous media. However, the influence of blowing or suction on the *vortex instability* of free or mixed convection flow in a porous medium seems not to have been investigated. This has motivated the present investigation. It should be noted that the corresponding problems for a viscous fluid on a concave and a horizontal wall were examined by Kobayashi [17] and Jang and Lie [18] respectively. As might be expected,

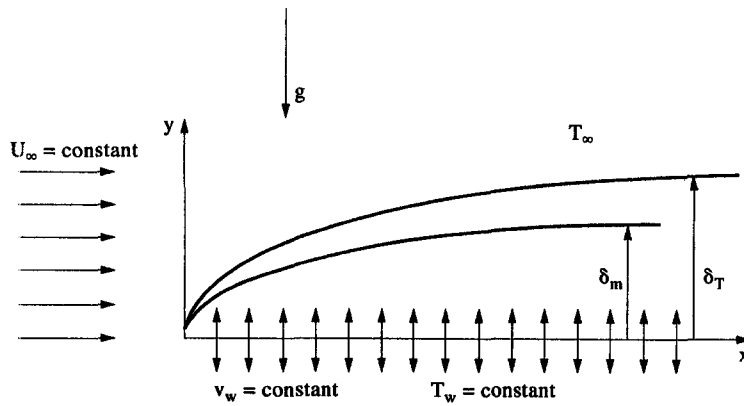


Fig. 1. Physical model.

$$\begin{aligned}
 x > 0 \quad y = 0 \quad T = T_w \quad V = V_w \\
 y \rightarrow \infty \quad T = T_\infty \\
 u = U_\infty
 \end{aligned} \tag{4}$$

where c is the inertia coefficient of the porous medium; K is the permeability of the saturated porous medium; β is the coefficient of thermal expansion; and α represents the equivalent thermal diffusivity. The other symbols are defined in the Nomenclature.

On introducing the following transformation :

$$\begin{aligned}
 \eta(x, y) = \frac{y}{x} Pe_x^{1/2} \quad \xi(x) = Pe_x^{1/2} \\
 f(\xi, \eta) = \frac{\psi(x, y)}{\alpha Pe_x^{1/2}} \quad \theta(\xi, \eta) = \frac{T - T_\infty}{T_w - T_\infty}
 \end{aligned} \tag{5}$$

where $Pe_x = U_\infty x / \alpha$, is the local Peclet number. Equations (1)–(3) can be non-dimensionalized as follows :

$$\begin{aligned}
 \frac{1}{\varepsilon} \frac{Pe_k^2}{\xi^2} f''' - (1 + Fr f') f' \\
 + M \left(\int_\eta^\infty \theta d\eta + \frac{1}{2} \xi \int_\eta^\infty \frac{\partial \theta}{\partial \xi} d\eta + \frac{1}{2} \eta \theta \right) = 0
 \end{aligned} \tag{6}$$

$$\theta'' = \frac{1}{2} \xi \left(f' \frac{\partial \theta}{\partial \xi} - \theta' \frac{\partial f}{\partial \xi} \right) - \frac{1}{2} f \theta' \tag{7}$$

with the prime denoting differentiation with respect to η . The corresponding boundary conditions are

$$\begin{aligned}
 f(\xi, 0) = f_w \quad f'(\xi, 0) = 0 \quad \theta(\xi, 0) = 1 \\
 f'(\xi, \infty) = 1 \quad \theta(\xi, \infty) = 0.
 \end{aligned} \tag{8}$$

It is noted that $M = Ra_x / Pe_x^{3/2}$ is the mixed convection parameter, which measures the importance of free to force convection. $M = 0$, corresponds to the case of purely force convection; while $M \rightarrow \infty$ corresponds to the case of purely free convection. $Fr = c U_\infty k^{1/2} / \nu$ is the Forchheimer number expressing the relative importance of the inertia effect and $Pe_k = U_\infty k^{1/2} / \alpha$

is the modified Peclet number; $f_w = -2v_w / U_\infty$ is the dimensionless blowing or suction parameters; f_w is positive for suction ($v_w < 0$), negative for blowing ($v_w > 0$), and $f_w = 0$ for the case of an impermeable surface [12]. It is noted that Darcy's law corresponds to the case of $Pe_k = 0$ and $Fr = 0$ [15].

It can be shown that the velocity components and the local Nusselt number can be expressed as

$$\begin{aligned}
 u &= U_\infty f' \\
 v &= -\alpha Pe_x^{1/2} \left(\frac{\partial \xi}{\partial x} \frac{\partial f}{\partial \xi} + \frac{1}{2x} f - \frac{\eta}{2x} f' \right) \\
 Nu_x / Pe_x^{1/2} &= -\theta'(\xi, 0).
 \end{aligned} \tag{9}$$

2.2. The disturbance flow

The standard method of linear stability theory is that in which the instantaneous values of the velocity, pressure and temperature are perturbed by small amplitude disturbances and the mean flow quantities are subtracted, with terms higher than first order in disturbance quantities being neglected. Then we get the following disturbance equations

$$\frac{\partial u_1}{\partial x} + \frac{\partial v_1}{\partial y} + \frac{\partial w_1}{\partial z} = 0 \tag{10}$$

$$\frac{\mu}{K} u_1 + \frac{c}{\sqrt{K}} \rho u_0 u_1 = -\frac{\partial p_1}{\partial x} + \frac{\mu}{\varepsilon} \nabla^2 u_1 \tag{11}$$

$$\frac{\mu}{K} v_1 + \frac{c}{\sqrt{K}} \rho u_0 v_1 = -\left(\frac{\partial p_1}{\partial y} - \rho_\infty g \beta T_1 \right) + \frac{\mu}{\varepsilon} \nabla^2 v_1 \tag{12}$$

$$\frac{\mu}{K} w_1 = -\frac{\partial p_1}{\partial z} + \frac{\mu}{\varepsilon} \nabla^2 w_1 \tag{13}$$

$$u_0 \frac{\partial T_1}{\partial x} + v_0 \frac{\partial T_1}{\partial y} + u_1 \frac{\partial T_0}{\partial x} + v_1 \frac{\partial T_0}{\partial y} = \alpha \nabla^2 T_1 \tag{14}$$

where the subscripts 0 and 1 signify the mean flow and disturbance components respectively, and σ is the ratio of volumetric heat capacity of the saturated porous medium to that of the fluid.

Following the method of order of magnitude analysis described in detail in [1], the terms $\partial u_1/\partial x$ and $\partial^2 T_1/\partial x^2$ in equations (10) and (14) can be neglected. The omission of $\partial u_1/\partial x$ in equation (10) implies the existence of a disturbance stream ψ_1 such that

$$w_1 = \frac{\partial \psi_1}{\partial y} \quad v_1 = -\frac{\partial \psi_1}{\partial z}. \tag{15}$$

We assume the three-dimensional disturbances for neutral stability are of the form

$$(\psi_1, u_1, T_1) = (\tilde{\psi}(x, y), \tilde{u}(x, y), \tilde{T}(x, y)) \exp [iaz] \tag{16}$$

where a is the spanwise periodic wave number. Substituting equation (16) into equations (10)–(14) and eliminating p_1 yields

$$\begin{aligned} \frac{\mu}{K} \left(ia\tilde{u} - \frac{\partial^2 \tilde{\psi}}{\partial x \partial y} \right) + \frac{c}{\sqrt{K}} ia\rho u_0 \tilde{u} \\ = \frac{\mu}{\varepsilon} \left(ia \frac{\partial^2 \tilde{u}}{\partial y^2} - ia\tilde{u} - \frac{\partial^4 \tilde{\psi}}{\partial x \partial y^3} + a^2 \frac{\partial^2 \tilde{\psi}}{\partial x \partial y} \right) \end{aligned} \tag{17}$$

$$\begin{aligned} \frac{\mu}{K} \left(\frac{\partial^2 \tilde{\psi}}{\partial y^2} - a^2 \tilde{\psi} \right) - \frac{c}{\sqrt{K}} a^2 \rho u_0 \tilde{\psi} = -ia\rho g\beta \tilde{T} \\ + \frac{\mu}{\varepsilon} \left(-2a^2 \frac{\partial^2 \tilde{\psi}}{\partial y^2} + a^4 \tilde{\psi} + \frac{\partial^4 \tilde{\psi}}{\partial y^4} \right) \end{aligned} \tag{18}$$

$$u_0 \frac{\partial \tilde{T}}{\partial x} + v_0 \frac{\partial \tilde{T}}{\partial y} + \tilde{u} \frac{\partial T_0}{\partial x} - ia\tilde{\psi} \frac{\partial T_0}{\partial y} = \alpha \left(\frac{\partial^2 \tilde{T}}{\partial y^2} - a^2 \tilde{T} \right). \tag{19}$$

Equations (17)–(19) are solved based on the local similarity approximations [1], wherein the disturbances are assumed to have weak dependence in the streamwise direction ($\partial/\partial x \ll \partial/\partial y$). Letting

$$\begin{aligned} F(\eta) = \frac{\tilde{\psi}(x, y)}{ia Pe_x^{1/2}} \quad G(\eta) = \frac{\tilde{u}(x, y)}{\alpha Pe_x^{1/2}/x} \\ \Theta(\xi, \eta) = \frac{\tilde{T}(x, y)}{(T_w - T_\infty)} \quad k = \frac{ax}{Pe_x^{1/2}} \end{aligned} \tag{20}$$

one gets the following system of equations for the local similarity approximation :

$$\begin{aligned} \frac{Pe_k^2}{\varepsilon} kG'' - \left(\xi^2 + Fr \xi^2 f' + \frac{Pe_k^2}{\varepsilon} k^2 \right) kG \\ = \frac{1}{2} \left(\xi^2 + Fr \xi^2 f' + \frac{Pe_k^2}{\varepsilon} \right) \eta F'' - \frac{Pe_k^2}{\varepsilon} F''' - \frac{1}{2} \frac{Pe_k^2}{\varepsilon} \eta F'''' \end{aligned} \tag{21}$$

$$\begin{aligned} \frac{Pe_k^2}{\varepsilon} F'''' - \left(\xi^2 + Fr \xi^2 f' + \frac{2Pe_k^2}{\varepsilon} k^2 \right) F'' \\ + \left(\xi^2 + Fr \xi^2 f' + \frac{Pe_k^2}{\varepsilon} k^2 \right) k^2 F = Mk \xi^3 \Theta \end{aligned} \tag{22}$$

$$\begin{aligned} \Theta'' + \frac{1}{2} \left(f + \xi \frac{\partial f}{\partial \xi} \right) \Theta' - \left(\frac{1}{2} f' + k^2 \right) \Theta \\ = \frac{1}{2\xi} \left(\theta + \xi \frac{\partial \theta}{\partial \xi} - \eta \theta' \right) G + k\xi \theta' F \end{aligned} \tag{23}$$

with the boundary conditions

$$\begin{aligned} F(0) = F'(0) = G(0) = \Theta(0) = 0 \\ F(\infty) = F'(\infty) = G(\infty) = \Theta(\infty) = 0. \end{aligned} \tag{24}$$

Equations (21)–(23) along with their boundary conditions, equation (24), constitute an eighth-order system of linear ordinary differential equations for the disturbance amplitude distributions $G(\eta)$, $F(\eta)$ and $\Theta(\eta)$. For fixed k , M , Fr , Pe_k and ε , the solutions G , F and Θ are eigenfunctions for the eigenvalue ξ .

3. NUMERICAL METHOD OF SOLUTION

In the stability calculations, the disturbance equations are solved by separately integrating four linearly independent integrals. The full solution may be written as the sum of four linearly independent solutions

$$\begin{aligned} G &= G_1 + E_2 G_2 + E_3 G_3 + E_4 G_4 \\ F &= F_1 + E_2 F_2 + E_3 F_3 + E_4 F_4 \\ \Theta &= \Theta_1 + E_2 \Theta_2 + E_3 \Theta_3 + E_4 \Theta_4. \end{aligned} \tag{25}$$

The four independent integrals (G_b , F_b , Θ_b) with $i = 1-4$ may be chosen so that their asymptotic solutions are

$$\begin{aligned} \Theta_1 &= \exp(\Gamma_1 \eta) & F_1 &= N_1 \exp(\Gamma_1 \eta) \\ \Theta_2 &= 0 & F_2 &= \exp(\Gamma_2 \eta) \\ \Theta_3 &= 0 & F_3 &= \exp(\Gamma_3 \eta) \\ \Theta_4 &= 0 & F_4 &= 0 \\ G_1 &= N_2 \exp(\Gamma_1 \eta) \\ G_2 &= N_3 \exp(\Gamma_2 \eta) \\ G_3 &= N_4 \exp(\Gamma_3 \eta) \\ G_4 &= \exp(\Gamma_3 \eta) \end{aligned} \tag{26}$$

where

$$\begin{aligned} \Gamma_1 &= \frac{1}{2} \left\{ -\frac{1}{2} \left(f + \xi \frac{\partial f}{\partial \xi} \right) \right. \\ &\quad \left. - \sqrt{\left[\frac{1}{2} \left(f + \xi \frac{\partial f}{\partial \xi} \right) \right]^2 + 4 \left(\frac{1}{2} + k^2 \right)} \right\} \end{aligned}$$

$$\Gamma_2 = -k$$

$$\Gamma_3 = -\sqrt{\frac{\varepsilon \xi^2}{Pe_k^2} + k^2}$$

$$N_1 = \frac{\varepsilon Mk \xi^3 / Pe_k^2}{\Gamma_1^4 + \frac{\varepsilon}{Pe_k^2} \left(\xi^2 + \frac{Pe_k^2 k^2}{\varepsilon} \right) k^2 - \frac{\Gamma_1^2 \varepsilon}{Pe_k^2} \left(\xi^2 + \frac{2Pe_k^2 k^2}{\varepsilon} \right)}$$

$$N_2 = \frac{\frac{\varepsilon}{Pe_k^2 k} \left[\frac{1}{2} \left(\xi^2 + \frac{Pe_k^2}{\varepsilon} \right) \eta N_1 \Gamma_1^2 - \frac{Pe_k^2}{\varepsilon} N_1 \Gamma_1^3 - \frac{1}{2} \frac{Pe_k^2}{\varepsilon} \eta N_1 \Gamma_1^4 \right]}{\Gamma_1^2 - \frac{\varepsilon}{Pe_k^2 k} \left(\xi^2 + \frac{Pe_k^2 k^2}{\varepsilon} \right) k}$$

$$N_3 = \frac{\frac{\varepsilon}{Pe_k^2 k} \left[\frac{1}{2} \left(\xi^2 + \frac{Pe_k^2}{\varepsilon} \right) \eta \Gamma_2^2 - \frac{Pe_k^2}{\varepsilon} \Gamma_2^3 \right]}{\Gamma_2^2 - \frac{\varepsilon}{Pe_k^2 k} \left(\xi^2 + \frac{Pe_k^2 k^2}{\varepsilon} \right) k}$$

$$N_4 = \frac{\frac{\varepsilon}{Pe_k^2 k} \left[\frac{1}{2} \left(\xi^2 + \frac{Pe_k^2}{\varepsilon} \right) \eta \Gamma_3^2 - \frac{Pe_k^2}{\varepsilon} \Gamma_3^3 - \frac{1}{2} \frac{Pe_k^2}{\varepsilon} \eta \Gamma_3^4 \right]}{(2 + \Gamma_3 \eta_\infty) \Gamma_3 - \frac{\varepsilon}{Pe_k^2 k} \left[\left(\xi^2 + \frac{Pe_k^2 k^2}{\varepsilon} \right) k \eta_\infty \right]}$$

An implicit finite-difference Keller Box method is used here to solve first the base flow system, equations (6) and (7), and the results are stored for a fixed step size, $\Delta\eta = 0.02$, which is small enough to permit accurate linear interpolation between the mesh points. Equations (21)–(23) with boundary conditions, equation (24), are then solved as follows. For specified k , ξ is guessed. Using equations (26) as starting values, the four integrals are integrated separately from the outer edge of the boundary layer to the wall using a sixth-order Runge–Kutta variable step-size integrating routine incorporated with the Gram–Schmidt orthogonalization procedure [19] to maintain the linear independence of the eigenfunctions. The required input of the base flow to the disturbance equations is calculated, as necessary, by linear interpolation of the stored base flow. From the values of the integrals at the wall, E_2 , E_3 and E_4 are determined using the boundary condition $G(0) = F(0) = \Theta(0) = 0$. The fourth boundary condition $F'(0) = 0$ is satisfied only for the appropriate value of the eigenvalue ξ . A Taylor series expansion of the initial guess of ξ provides a correction scheme for the initial guess of ξ . Iterations continue until the second boundary condition is sufficiently close to zero ($< 10^6$, typically).

4. RESULTS AND DISCUSSIONS

Numerical results for the velocity, temperature profiles, Nusselt number, the critical Peclet number and wave numbers at the onset of vortex instability are

presented for mixed convection parameter $M = 0.1$ –2 with the dimensionless blowing or suction parameter f_w ranging from -1 to 1.0 . In order for the boundary layer assumptions ($v \ll u$) to be valid in the present analysis, the values of f_w are limited in the range of -1 to 1 .

Figure 2 show the velocity and temperature profiles across the boundary layer for selected values of f_w ($-1, -0.5, 0, 0.5$ and 1.0) and for $M = 1$. The velocity profiles are referred to the left and lower axes, while the temperature profiles are referred to the right and

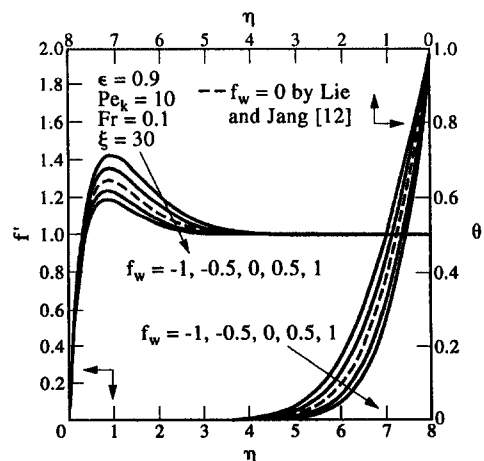


Fig. 2. Tangential velocity and temperature profiles across the boundary layer for selected values of f_w for $M = 1$.

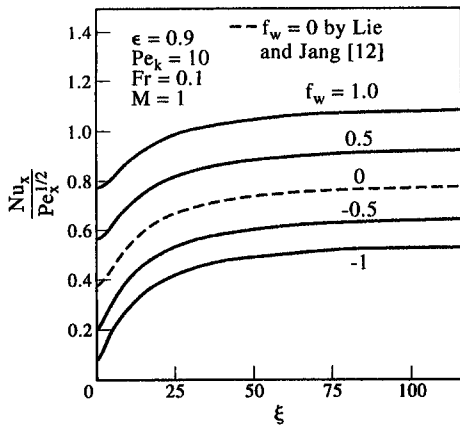


Fig. 3. Alternation of $Nu_x/Pe_x^{1/2}$ with ξ for various values of f_w .

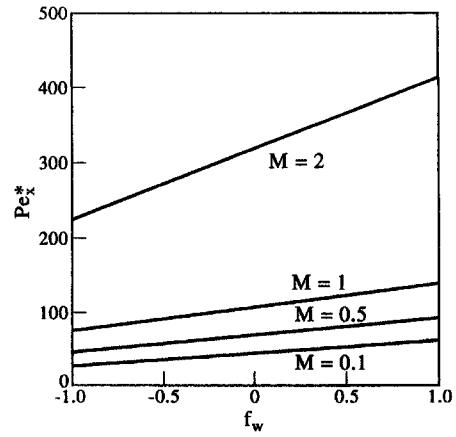


Fig. 5. Critical Peclet number as a function of f_w for various values of M .

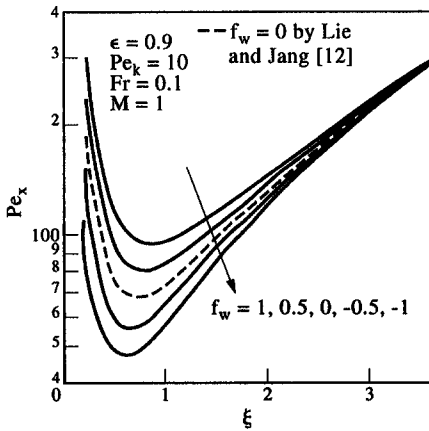


Fig. 4. Neutral stability curves for various values of f_w for $M = 1$.

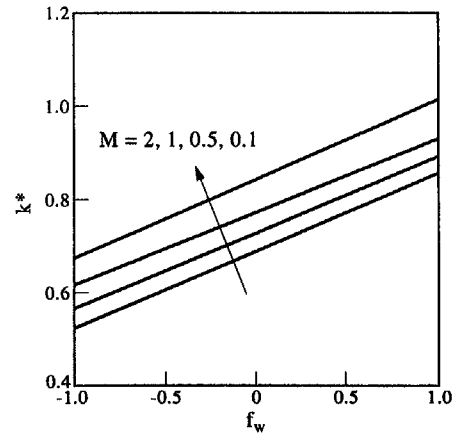


Fig. 6. Critical wave number as a function of f_w for various values of M .

upper axes. It should be noted that $f_w = 0$ represents the flow over an impermeable surface [12]. The values of $f_w < 0$ correspond to blowing, while the values of $f_w > 0$ correspond to suction. It is seen from Fig. 2 that the blowing or suction markedly affects the velocity and temperature fields. It is seen that surface blowing ($f_w < 0$) tends to increase both the tangential velocity and temperature boundary layer thicknesses, while they are decreased for surface suction ($f_w > 0$). Figure 3 shows the alternation of $Nu_x/Pe_x^{1/2}$ with ξ for various values of blowing/suction parameter f_w . One can see that blowing ($f_w < 0$) decreases the heat transfer rate, while suction ($f_w > 0$) increases it. For suction, the fluid at the ambient temperature is brought closer to the surface resulting in a decrease of the thermal boundary layer thickness and an increase of the heat transfer rate. On the other hand, for blowing, the ejected fluids forms a thick buffer layer against which heat must transfer by conduction resulting in a drop in the heat transfer rate.

Figure 4 show the neutral stability curves, in terms of Pe_x and dimensionless wave number k , for various

values of dimensionless blowing or suction parameter f_w ($-1, -0.5, 0, 0.5$ and 10) and for $M = 1$. It is observed that, for suction ($f_w > 0$), as f_w increases (i.e. stronger suction), the neutral stability curves shift to higher Rayleigh number and higher wave number, indicating a stabilization of the flow to the vortex instability, while for blowing ($f_w < 0$), as $|f_w|$ increases (i.e. stronger blowing) the neutral stability curves shift to the lower Rayleigh number and lower wave number, indicating a destabilization of the flow.

The critical Peclet number Pe_x and the critical wave number k , which marks the onset of longitudinal vortices, can be found from the minimum of the neutral stability curves. The critical Peclet number and wave number are plotted as a function of dimensionless blowing and suction parameter f_w in Figs. 5 and 6, respectively, for various values of mixed convection parameter M . The results indicate that suction ($f_w > 0$) tends to stabilize the flow, while blowing ($f_w < 0$) tends to destabilize it. The reason that suction is more stable is due to the fact that the effect of

suction is to suck away the warm fluid on the plate and suppress the occurrence of vortices, and consequently suction stabilizes the vortex mode of instability. It is apparent from Fig. 6 that the critical wave number increases as the flow changes from strong blowing to strong suction (i.e. f_w increases). Finally, a close look of Figs. 5 and 6 indicates that the effects of mixed convection parameter M on the critical Peclet number and critical wave number are more pronounced than the effect of dimensionless suction or blowing parameter f_w .

5. CONCLUSIONS

The effects of uniform surface blowing or suction on the vortex instability of a horizontal mixed convection boundary layer flow in a saturated porous medium have been examined by a linear stability theory. The numerical results demonstrate that blowing ($f_w < 0$) reduces the heat transfer rate and destabilizes the flow as compared with the case of an impermeable surface, while for suction ($f_w > 0$), the opposite trend is true. It is also found that the critical wave number increases as the flow changes from strong blowing to strong suction.

Acknowledgement—Financial support was provided by the National Science Council of the Republic of China under contract NSC 79-0401-E006-06.

REFERENCES

1. C. T. Hsu, P. Cheng and G. M. Homsy, Instability of free convection flow over a horizontal impermeable surface in a porous medium, *Int. J. Heat Mass Transfer* **21**, 1221–1228 (1978).
2. C. T. Hsu and P. Cheng, Vortex instability in buoyancy-induced flow over inclined heated surfaces in a porous media *J. Heat Transfer* **101**, 660–665 (1979).
3. J. Y. Jang and W. J. Chang, Vortex instability of buoyancy-induced inclined boundary layer flow in a saturated porous medium, *Int. J. Heat Mass Transfer* **31**, 759–767 (1988).
4. J. Y. Jang and W. J. Chang, The flow and vortex instability of horizontal natural convection in a porous medium resulting from combined heat and mass buoyancy effect, *Int. J. Heat Mass Transfer* **31**, 769–777 (1988).
5. J. Y. Jang and W. J. Chang, Vortex instability of inclined buoyant layer in porous media saturated with cold water, *Int. Commun. Heat Mass Transfer* **14**, 405–416 (1987).
6. J. Y. Jang and W. J. Chang, Maximum density effects on vortex instability of horizontal and inclined buoyancy-induced flows in porous media, *J. Heat Transfer* **111**, 572–574 (1989).
7. W. J. Chang and J. Y. Jang, Inertia effects on vortex instability of a horizontal natural convection flow in a saturated porous medium, *Int. J. Heat Mass Transfer* **32**, 541–550 (1989).
8. W. J. Chang and J. Y. Chang, Non-Darcian effects on vortex instability of a horizontal natural convection flow in a porous medium, *Int. J. Heat Mass Transfer* **32**, 529–539 (1989).
9. C. T. Hsu and P. Cheng, Vortex instability of mixed convective flow in a semi-infinite porous medium bounded by a horizontal surface, *Int. J. Heat Mass Transfer* **23**, 789–798 (1980).
10. C. T. Hsu and P. Cheng, The onset of longitudinal vortices in mixed convective flow over an inclined surface in a porous medium, *J. Heat Transfer* **102**, 544–549 (1980).
11. J. Y. Jang and K. N. Lie, Vortex instability of mixed convection flow over horizontal and inclined surfaces in a porous medium, *Int. J. Heat Mass Transfer* **35**, 2077–2085 (1992).
12. K. N. Lie and J. Y. Jang, Boundary and inertia effects on vortex instability of a horizontal mixed convection flow in a porous medium, *Numer. Heat Transfer, A* **23**, 361–378 (1993).
13. P. Cheng, The Influence of Lateral Mass Flux on Free Convection Boundary Layers in a Saturated Porous Medium, *Int. J. Heat Mass Transfer*, **20**, 201–206 (1977).
14. W. J. Minkowycz, P. Cheng and F. Moalem, The effect of surface mass transfer on buoyancy-induced Darcian flow adjacent to a horizontal heated surface, *Int. Commun. Heat Mass Transfer* **12**, 55–65 (1985).
15. F. C. Lai and F. A. Kulacki, The influence of surface mass flux on mixed convection over horizontal plates in saturated porous media, *Int. J. Heat Mass Transfer* **33**, 576–579 (1990).
16. F. C. Lai and F. A. Kulacki, The influence of lateral mass flux on mixed convection over inclined plates in saturated porous media, *J. Heat Transfer* **112**, 515–518 (1990).
17. R. Kobayashi, Note on the stability of a boundary layer on a concave wall with suction, *J. Fluid Mech.* **52**, 269–272 (1972).
18. J. Y. Jang and K. N. Lie, Effects of blowing/suction on vortex instability of horizontal free convection flows, *AIAA J. Thermophys.* **7**, 749–751 (1993).
19. A. R. Wazzan, T. T. Okamura and A. M. O. Smith, Stability of laminar boundary layers at separation, *Phys. Fluids* **10**, 2540–2545 (1967).